DESIGN AND ANALYSIS OF EMBEDDED I&C FOR LOOP-SCALE MAGNETICALLY SUSPENDED PUMP

Alexander M. Melin and Roger A. Kisner*
Oak Ridge National Laboratory
1 Bethel Valley Road
Oak Ridge, TN 37831
melina@ornl.gov; kisnerra@ornl.gov

ABSTRACT

Improving nuclear reactor designs and fuel processing technologies for safer and more efficient operation require the development of new component designs. In particular, many of the advanced reactor design such as the molten salt reactors and high-temperature gas cooled reactors have operating environments beyond the ability of many currently commercially available components. To address this, new cross-cutting technologies need to be developed that will enable the design, fabrication, and reliable operation of new classes of reactor components. The Advanced Sensor Initiative of the Nuclear Energy Enabling Technologies initiative is investigating advanced sensor and control designs that are capable of operating in these extreme environments. Under this initiative Oak Ridge National Laboratory (ORNL) has been developing embedded instrumentation and control for extreme environments. To develop, test, and validate these new sensing and control techniques, ORNL is building a pump testbed with submerged magnetic bearings. The eventual goal is to apply these techniques to a high temperature (700 °C) canned rotor pump that utilizes active magnetic bearings to eliminate the need for mechanical bearings and seals. The technologies will benefit the Next Generation Power Plant, Advanced Reactor Concepts, and Small Modular Reactor programs. In this paper we will detail the design and analysis of the embedded I&C testbed with submerged magnetic bearings. Then we will analyze the fluid forces on the shaft. Finally, we will develop the radial and thrust bearing geometries needed to meet the force requirements.

Key Words: Embedded I&C, Active Magnetic Bearings, Advanced I&C, Extreme Environments, Pumps

1 INTRODUCTION

Improving nuclear reactor safety, efficiency, and cost are necessary to their continued use as an important generation source. Often times, these improvements require that the reactors operate in extreme environments not seen in current designs. These extreme environments can include high temperatures, high pressures, corrosive environments, and high radiation. In these new extreme operating environments, many current component designs will not provide sufficient safety, performance, and reliability. In fact, many existing component technologies will not function in these new environments. To meet the safety and performance goals, new cross-cutting technologies need to be developed for instrumentation and control that can operate in these extreme environments.

The Advanced Sensors Initiative (ASI), a subprogram of the Department of Energy's Nuclear Energy Enable Technologies (NEET) initiative is funding research into new cross-cutting technologies to enable new classes of reactor components that will overcome the challenges of operating in extreme environments. In particular, the ASI program is focusing on new sensor and control techniques including embedded instrumentation and control (I&C). Under this program, Oak Ridge National Laboratory (ORNL) is investigating high temperature (700 °C) magnetic bearings for use in reactor components such as fluid pumps and turbines. The use of active magnetic bearings in a pump would remove the need for mechanical bearings and seals that are the main cause of maintenance costs and failures.[14, 4, 2, 13] Currently ORNL is researching advanced instrumentation and control for room temperature magnetic bearings using materials and designs similar to a conceptual high-temperature canned rotor pump created by ORNL[6] to develop the foundational technologies needed for high temperature operation. This includes modeling, closed-loop system identification, sensorless operations, and advanced control strategies in conjunction with material, mechanical, electromagnetic, and electromechanical design.

The initial phase of the project looked at materials, sensors, and control techniques to develop a conceptual high-temperature canned rotor pump (i.e. the internal components of the pump are in direct contact with the pumped fluid and protected by a barrier material) with magnetic bearings.[6, 8, 11, 5] This phase of the project also developed detailed models of the electromagnetics and rotordynamics including the nonlinear hydrodynamic forces in the fluid gap between the rotor and stator.[12] Commercial magnetic bearings do not experience these larger fluid forces because they operate in air or vacuum. For example, they are commonly used in aerospace gyroscopes, momentum wheels, and vacuum turbopumps to name a few.

The next phase of the project was the creation of a laboratory scale magnetic bearing testbed. This testbed was used to investigate closed-loop system identification techniques, develop stabilizing controllers, validate models, and create software toolsets for the design and analysis of magnetic bearing geometries and controls.[10]

The third phase of the project that is currently underway is the development of a submerged magnetic bearing testbed.[9] As far as the authors are aware, this will be the first magnetic bearing to operate submerged in fluid. The SKF company has built an undersea gas compression system that uses magnetic bearings, but they are not in contact with the surrounding seawater. The submerged magnetic bearing testbed will be a fully operational water pump with a shaft that is levitated using two radial and two omnidirectional thrust magnetic bearings. The goal of the testbed is to develop an embedded instrumentation and control system that can stabilize the shaft the the presence of the additional nonlinear fluid effects including speed dependent Taylor-Couette flow bifurcation.[3] The rest of this paper will provide details of the submerged magnetic bearing testbed design.

2 DESIGN CONCEPT

To reduce the cost and time needed to design and fabrication an induction motor driven pump, a commercial canned rotor pump was chosen to be the foundation of the testbed. Canned rotor pumps operate with the rotor and stator submerged in the pumped fluid and utilize a thin metal 'can' around the electromagnetic components to prevent their contact with the fluid. The pump chosen was a Teikoku 204TF1 impeller pump. The nominal pump flow rate at 3450 RPM is 511 L/min with a nominal head of 75 m. To create the testbed, the original pump will be retrofitted with active magnetic bearings that will replace the existing graphite fluid bearings. This requires extensive modification to the original pump but allows the use of the existing 3600 RPM induction motor, impeller, and volute. Since detailed manufacturing drawings of the Teikoku

pump were not available, the pump was disassembled then each component was measured and modeling in 3D. The solid model of the unmodified pump is shown in figure 1 without the volute. After the development

Figure 1. 3D Model of the Teikoku 204TF1 pump created after disassembly and measurement.

of an accurate solid model of the original pump, the design was modified to add two radial and two omnidirectional thrust magnetic bearings at each end of the shaft. The original pump shaft is extended to include the radial bearing magnetic laminations and thrust bearing magnetic core. While the original induction motor is canned, the magnetic bearing designs are not canned and are in direct contact with the pumped fluid. Isolation feedthroughs are used for both the magnetic coil power and inductive position sensor signals.

Figure 2 shows the final design of the modified Teikoku 204TF1 pump and figure 3 shows a closer view of the front magnetic bearing.

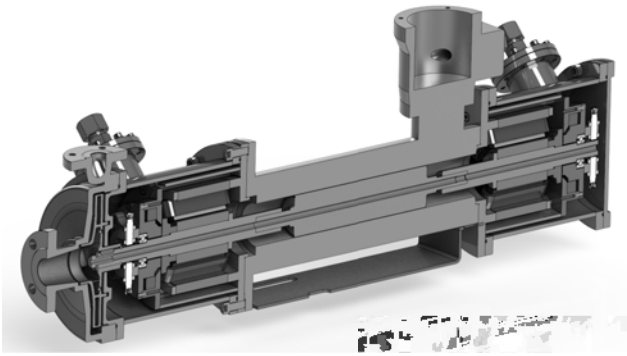

Figure 2. 3D Model of the modified Teikoku 204TF1 pump magnetic bearing testbed.

3 IMPELLER FORCES

The active magnetic bearings must have sufficient force capacity to overcome any shaft forces over the full range of the shaft movement ($\pm$ 0.75 mm). The primary forces on the shaft are due to gravity, fluid forces on the impeller, and position dependent fluid forces on the shaft. The operating condition of the

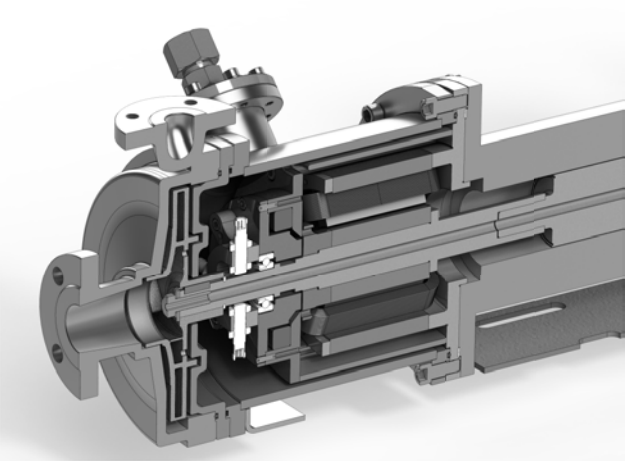

Figure 3. Closer view of the combined front thrust and radial magnetic bearings.

pump defines the fluid forces acting on the impeller. The Teikoku 204TF1 impeller has a single volute design, closed impellers, balance holes, and a back ring.

The radial loading of the pump is affected by the volute design and the fraction of operating capacity (how far from the best efficiency point (BEP)) the pump is operating at. The radial load is given by

$$F_r = \frac{K_r H D B S_G}{1.02 \times 10^{-4}} \tag{1}$$

where K_r is a radial thrust factor, H is the impeller head at the flow point in m, D is the impeller diameter in m, and B is the impeller width at the vane discharge including the shroud in m and S_G is the specific gravity of the fluid being pumped [7]. Table I summarizes the relevant physical parameters and radial forces on the Teikoku 204TF1 pump with the minimum and maximum expected values.

Table I. Teikoku 204TF1 Radial Forces

Parameter	Value	Units
K_r	(0.09, 0.38)	
H	(54.9, 88.4)	m
D	0.208	m
B	0.0158	m
S_G	1.0	
F_r	(159.2, 1082.3)	N

The axial loading of the pump is affected by the pump flow rate and the pressure differential created between the front and rear of the impeller and the impeller design [7]. The manufacturer of the pump tests the axial force for their different models and supplied test data for the Teikoku 204TF1 shown in Figure 4

The maximum measured axial force for the 0.208 m (8.188 in) diameter impeller is 510 N (52 kgf) which is below the maximum allowable force specified by the manufacturer of 600 N.

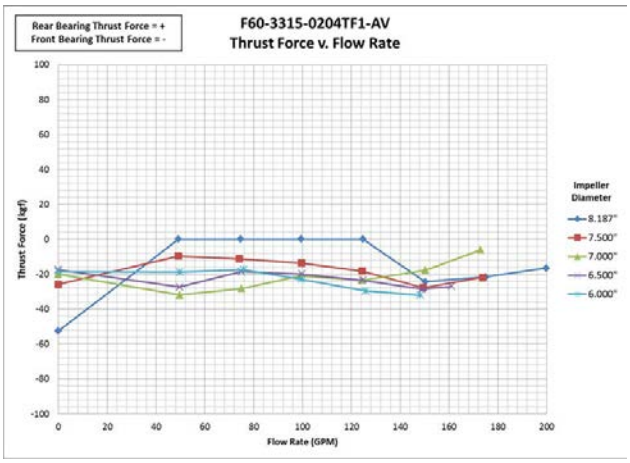

Figure 4. Axial force test data for a Teikoku canned rotor pump from the manufacturer.

4 RADIAL BEARING

The forces on both radial bearings due to fluid forces on the impeller can be calculated based on the distances from the impeller to the bearings. We will denote the impeller as the 'front' of the pump, the $Z+$ direction from the center of mass towards the impeller, and the radial bearing that is the closest to the impeller as the front bearing or bearing A. The bearing furthest from the impeller will be denoted as the rear bearing or bearing B. The distance from bearing A to the impeller outlet denoted by L_A is approximately 0.27 m and the distance from bearing B to the impeller outlet denoted by L_B is approximately 0.860 m.

Using the following equations, the reaction forces at the bearings F_A and F_B can be calculated.

$$F_A = F_r - F_B \tag{2}$$

$$F_B = F_r \frac{L_A}{L_B} \tag{3}$$

Given a maximum radial force of $F_r = 1082\ N$, bearing A will support 742 N and bearing B will support 339 N. The bearing windings will use 16 AWG wire which has a nominal current limit of 20 A which will maintain a reasonable temperature in atmosphere. Based on these current and load parameters, both front and rear radial bearings will be designed to create 2000 N force at 10 A when the shaft is centered in the stator.

The radial magnetic bearings will use a differential bearing driving mode. The force created by the radial magnetic bearing can be calculated for a rotor position x and control current u_i by[15, 1]

$$F = k\left(\frac{(i_0 + u_i)^2}{(x_0 - x)^2} - \frac{(i_0 - u_i)^2}{(x_0 + x)^2}\right)\cos\alpha \tag{4}$$

with

$$k = \frac{1}{4}\mu_0 N^2 A_R \tag{5}$$

Figure 5 shows both the theoretical linearized force characteristics of the radial bearing differential drive design along with the nonlinear force calculated using the material properties of M19 electrical steel which

Table II. Radial Bearing Geometry

Parameter	Value	Units	Description
x_0	0.0015	m	Air Gap
i_0	8.0	A	Bias Current
d_r	0.066	m	Rotor OD
h_t	0.030	m	Tooth Height
w_t	0.0129	m	Tooth Width
h_s	0.100	m	Stack Height
N	160	$turns$	Total Coil Turns
α	22.5°	deg	Tooth Angle

is used for the rotor and stator laminations in the radial bearings. Linearizing (4) about the operating points $x = 0$ and $u_i = 0$ yields the expression of the bearing force given by[15, 1]

$$F_l = k_i i + k_x x \tag{6}$$

where

$$k_i = \frac{4ki_0}{x_0^2} \tag{7}$$

$$k_x = \frac{4ki_0^2}{x_0^3} \tag{8}$$

For this radial bearing design, $k_i = 136.3$ and $k_x = 727044.6$.

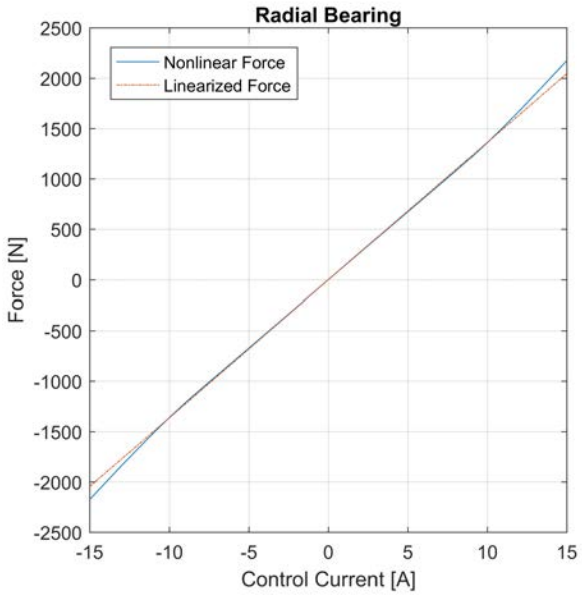

Figure 5. Radial bearing nonlinear force for M19 steel when the rotor is in the center of the stator.

We also need to ensure that the bearing will have sufficient force at the limits of the radial motion to overcome weight of the shaft. The shaft has a mass of $18.3391\ kg$ and a weight of $180\ N$. Figure 6

shows the nonlinear force produced by the radial bearing when it is resting on the touchdown bearings and demonstrates that the radial bearing will have sufficient force magnitudes at the limits of shaft travel to overcome the gravitational forces on the shaft.

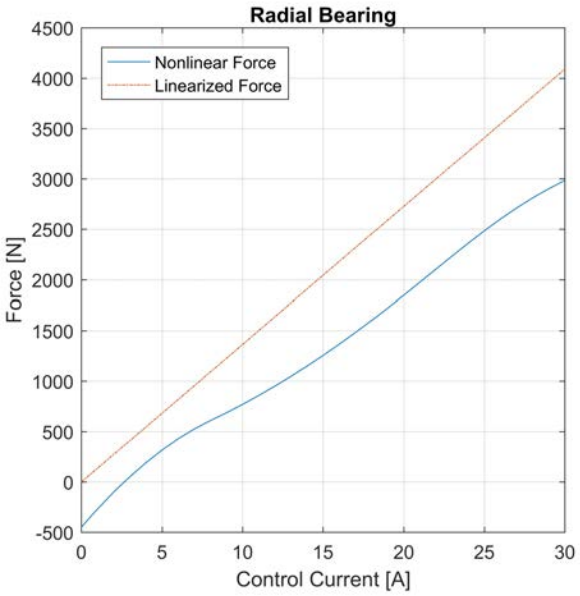

Figure 6. Radial bearing nonlinear for for M19 steel when the rotor is at the limit of its motion.

5 AXIAL BEARING

The axial bearing will have two concentric annulus surfaces on the stator for the flux to pass through to the rotor. To maximize the magnetic flux, the area of both of these annulus should be equal. In addition, we would like to separate the outer diameter of the smaller annulus and the inner diameter of the larger annulus by a gap larger than the thrust bearing airgap to reduce the magnetic forces between them and prevent a short circuit of the magnetic flux. Given the outer radius of the larger annulus r_o, the inner radius of the smaller annulus r_i, and the gap g_a we can calculate the smaller annulus outer radius r_i^m and the larger annulus inner radius $r_o^m = r_i^m + g_a$.

$$r_i^m = \frac{1}{2}\left(-1 + \sqrt{2r_i^2 + 2r_0^2 - 2g_a + 1}\right) \tag{9}$$

For the Teikoku pump, we will choose a $r_o = 43\ mm$, $r_o^m = 34.2\ mm$, $r_i^m = 32.2\ mm$, and $r_i = 17\ mm$ for a 2 mm gap. This give a cross sectional area of 2350 mm^2. Assuming a maximum flux density B_{max} of 1.4 T, the maximum force that can be created by the impeller side axial magnetic bearing is

$$F_{max} = \frac{B_{max}^2 A_T}{\mu_0} = 3328\ N \tag{10}$$

and the number of windings N_T to achieve the maximum magnetic flux is

$$N_T = \frac{2B_{max} z_0}{\mu_0 u_i} = 334\ turns \tag{11}$$

where $z_0 = 1.5\ mm$ is the nominal airgap and $u_i = 10\ A$ is the nominal coil current. With 16 AWG wire with a cross sectional area of 1.3 mm^2 and a packing factor of 0.6, the required winding area is 868 mm^2.

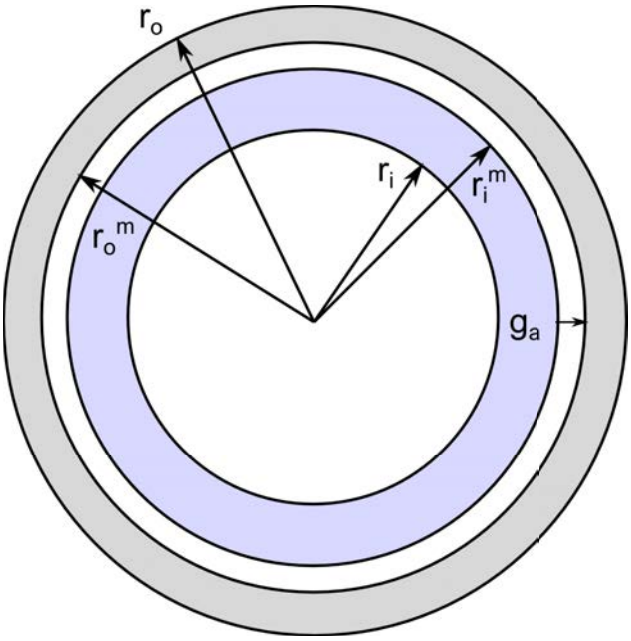

Figure 7. Thrust bearing annuli and geometric quantities.

With a bias current of 3.5 A and an airgap of 1.5 mm, the thrust bearing has the linearized coefficients

$$k_i = 465.4$$
$$k_x = 1085963$$

Figure 8 shows the nonlinear force when using M19 steel and the linearized force for the thrust bearing in bipolar mode. The maximum nonlinear force corresponds to the theoretical maximum force calculated in (10). Figure 9 shows the force response of the thrust bearing at the limit of the shaft travel. This figure shows that even at the limit of travel, the thrust bearing creates enough force to overcome the maximum expected axial force of 600 N.

6 CONCLUSIONS

The development of embedded instrumentation and controls for submerged active magnetic bearing will expand the operating environments that existing commercial magnetic bearings operate in. The primary difficulty is the increased shaft forces caused by the impeller and other nonlinear fluid effective such as the Taylor-Couette flow bifurcation. The control design will need to maintain stable operation over a range of frequencies and forces. The development of I&C for submerged magnetic bearings is also a step towards the development of high-temperature magnetic bearings that can maintain contact with high temperature fluids such as molten salts that are the primary coolant in molten salt reactors. The instrumentation and control along with the ancillary technologies and fabrication techniques developed during this research will benefit multiple reactor classes and designs.

7 ACKNOWLEDGMENTS

This work was sponsored by the US Department of Energy (DOE) Nuclear Energy Enabling Technologies (NEET) program on Advanced Sensors and Instrumentation (ASI).

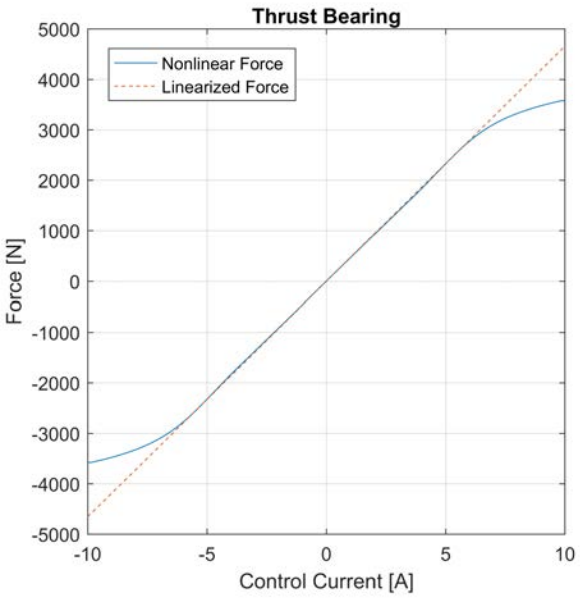

Figure 8. Thrust bearing force when centered.

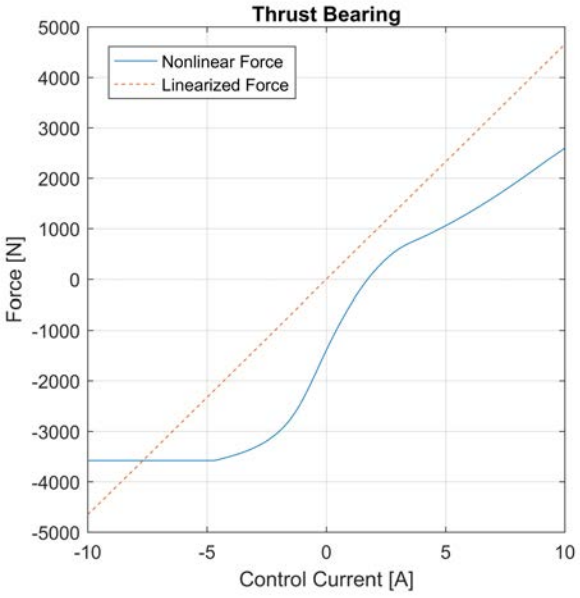

Figure 9. Thrust bearing force at the limit of travel.

8 REFERENCES

1. A. Chiba, T. Fukao, O. Ichikawa, M. Oshima, M. Takemoto, and D. G. Dorrell, *Magnetic Bearings and Bearingless Drives*. Elsevier, 2005.

2. D. R. Diercks, "Analysis of failed nuclear plant components," *Materials Engineering and Performance*, vol. **2**, no. 6, pp. 799–806, 1993.

3. H.-S. Dou, B. C. Khoo, and K. S. Yeo, "Instability of taylor-couette flow between concentric rotating cylinders," *Int. J. of Thermal Science*, vol. **47**, no. 11, pp. 1422–1435, November 2008.

4. J. E. Jackson, "Draft regulatory guide dg-1008 reactor coolant pump seals," NRC, Tech. Rep. DG-1008, 1991.

5. R. A. Kisner, D. L. Fugate, A. M. Melin, D. E. Holcomb, D. F. Wilson, P. C. Silva, and C. C. Molina, "Evaluation of manufacturability of embedded sensors and controls with canned rotor pump system," Oak Ridge National Laboratory ORNL/TM-2013/269, Tech. Rep., 2013.

6. R. A. Kisner, A. M. Melin, T. A. Burress, D. L. Fugate, D. E. Holcomb, J. B. Wilgen, J. M. Miller, D. F. Wilson, P. C. Silva, L. J. Whitlow, and F. J. Peretz, "Embedded sensors and controls to improve component performance and reliability: Conceptual design report," Oak Ridge National Laboratory ORNL/TM-2012/433, Tech. Rep., 2012.

7. V. S. Lobanoff and R. R. Ross, *Centrifugal Pumps Design & Application*. Gulf Publishing Company, 1985.

8. A. M. Melin, R. Kisner, and D. L. Fugate, "Embedded sensors and controls to improve component performance and reliability: System dynamics modeling and control system design," Oak Ridge National Laboratory, Tech. Rep. ORNL/TM-2013/415, 2013.

9. A. M. Melin and R. A. Kisner, "Embedded sensors and controls to improve component performance and reliability - loop-scale testbed design report," Oak Ridge National Laboratory, Tech. Rep. ORNL/TM-2016/563, 2016.

10. A. M. Melin, R. A. Kisner, A. Drira, and F. K. Reed, "Embedded sensors and controls to improve component performance and reliability - bench-scale testbed design report," Oak Ridge National Laboratory, Tech. Rep. ORNL/TM-2015/584, 2015.

11. A. M. Melin, R. A. Kisner, and D. L. Fugate, "Advanced instrumentation and controls for extreme environments," *IEEE Instrumentation and Measurement Magazine*, vol. **16**, no. 3, June 2013.

12. A. M. Melin, R. A. Kisner, D. L. Fugate, and D. E. Holcomb, "Hydrodynamic effects on modeling and control of a high temperature active magnetic bearing pump with a canned rotor," in *NPIC&HMIT*, 2015.

13. P. S. Pickard, "Sodium reactor experiment accident july 1959," 2009.

14. S. K. Shaukat, J. E. Jackson, and D. F. Thatcher, "Regulatory analysis for generic issue 23: Reactor coolant pump seal failure," IAEA, Tech. Rep. NUREG-1401, 1991.

15. A. Traxler and E. Maslen, *Magnetic Bearings: Theory, Design, and Application to Rotating Machinery*. Springer, 2010.